

Permanent Neonatal Diabetes in *INS*^{C94Y} Transgenic Pigs

Simone Renner,¹ Christina Braun-Reichhart,¹ Andreas Blutke,³ Nadja Herbach,³ Daniela Emrich,³ Elisabeth Streckel,¹ Annegret Wünsch,¹ Barbara Kessler,¹ Mayuko Kurome,^{1,5} Andrea Bähr,¹ Nikolai Klymiuk,¹ Stefan Krebs,² Oliver Puk,⁴ Hiroshi Nagashima,⁵ Jochen Graw,⁴ Helmut Blum,² Ruediger Wanke,³ and Eckhard Wolf^{1,2,5}

Mutations in the insulin (*INS*) gene may cause permanent neonatal diabetes mellitus (PNDM). *Ins2* mutant mouse models provided important insights into the disease mechanisms of PNDM but have limitations for translational research. To establish a large animal model of PNDM, we generated *INS*^{C94Y} transgenic pigs. A line expressing high levels of *INS*^{C94Y} mRNA (70–86% of wild-type *INS* transcripts) exhibited elevated blood glucose soon after birth but unaltered β -cell mass at the age of 8 days. At 4.5 months, *INS*^{C94Y} transgenic pigs exhibited 41% reduced body weight, 72% decreased β -cell mass (–53% relative to body weight), and 60% lower fasting insulin levels compared with littermate controls. β -cells of *INS*^{C94Y} transgenic pigs showed a marked reduction of insulin secretory granules and severe dilation of the endoplasmic reticulum. Cataract development was already visible in 8-day-old *INS*^{C94Y} transgenic pigs and became more severe with increasing age. Diabetes-associated pathological alterations of kidney and nervous tissue were not detected during the observation period of 1 year. The stable diabetic phenotype and its rescue by insulin treatment make the *INS*^{C94Y} transgenic pig an attractive model for insulin supplementation and islet transplantation trials, and for studying developmental consequences of maternal diabetes mellitus. *Diabetes* 62:1505–1511, 2013

Heterozygous mutations of the insulin (*INS*) gene have been identified as a cause of permanent neonatal diabetes mellitus (PNDM) in humans (1). *Ins2*^{+C96Y} (Akita) and Munich *Ins2*^{+C95S} mutant mice have development of hyperglycemia early in life, reduced insulin secretion after glucose challenge, ultrastructural β -cell alterations, and progressive β -cell loss (2,3). These models contributed substantially to the clarification of disease mechanisms induced by misfolded (pre)proinsulin, including impaired trafficking of normal proinsulin by formation of high-molecular-weight complexes with mutant (pro)insulin (4), accumulation of misfolded insulin in the endoplasmic reticulum (ER), and ER stress (5). ER stress triggers β -cell apoptosis and diabetes mellitus when it exceeds a certain level (6). Although there is increased degradation of misfolded insulin molecules (7), β -cell failure finally occurs.

From the ¹Chair for Molecular Animal Breeding and Biotechnology, Ludwig Maximilian University Munich, Munich, Germany; the ²Laboratory for Functional Genome Analysis, Gene Center, Ludwig Maximilian University Munich, Munich, Germany; the ³Institute of Veterinary Pathology at the Centre for Clinical Veterinary Medicine, Ludwig Maximilian University Munich, Munich, Germany; the ⁴Helmholtz Center Munich-German Research Center for Environmental Health, Institute of Developmental Genetics, Neuherberg, Germany; and the ⁵Meiji University, International Institute for Bio-Resource Research, Kawasaki, Japan.

Corresponding author: Eckhard Wolf, ewolf@lmb.uni-muenchen.de.

Received 7 August 2012 and accepted 7 November 2012.

DOI: 10.2337/db12-1065

© 2013 by the American Diabetes Association. Readers may use this article as long as the work is properly cited, the use is educational and not for profit, and the work is not altered. See <http://creativecommons.org/licenses/by-nc-nd/3.0/> for details.

Whereas *Ins2* mutant mouse models provided important mechanistic insights, they have limitations for translational studies. To establish a large animal model of PNDM, we generated transgenic pigs expressing a mutant porcine *INS* gene (*INS*^{C94Y}) that resembles the human *INS*^{C96Y} mutation and the mutation of the Akita mouse.

RESEARCH DESIGN AND METHODS

Generation of *INS*^{C94Y} transgenic pigs. All animal experiments were performed according to the German Animal Welfare Act with permission of the responsible animal welfare authority. The *INS*^{C94Y} expression vector including the porcine *INS* gene with the G→A transition leading to a Cys→Tyr exchange at amino acid position 94 as well as its essential regulatory elements and a neomycin selection cassette (neo) (Fig. 1A) were nucleofected into male primary porcine fetal fibroblasts, and pools of stable nucleofected cell clones were used for nuclear transfer to generate transgenic founder pigs (8). Genotyping was performed by PCR using the transgene-specific primers 5'-CAG CTG TGC TCG ACG TTG TC-3' and 5'-GAG TCA ACT AGT CCT CAG AAG AAA G-3', and Southern blot analysis using a ³²P-CTP-labeled probe specific for the neo cassette (Fig. 1B). For transgene expression studies, total RNA was extracted from pancreatic tissue (RNeasy Kit; Qiagen), DNaseI-treated (Roche), and reverse-transcribed with SuperScriptII (Life Technologies) using random hexamer primers. *INS*^{C94Y} and wild-type *INS* cDNAs were amplified by PCR using insulin-specific primers 5'-TTT TTA TCC GCA TTC TTA CAC GG-3' and 5'-ATC TTC CTC AGC TCC TTC CAG G-3', and their ratio was determined by next-generation sequencing of RT-PCR amplicons (Genome Analyzer IIx; Illumina; >10,000 reads per sample).

Animal husbandry, in vivo parameters, and insulin treatment. Animals were housed under controlled conditions, had a once-daily feeding regimen, and had free access to water. Body weight was recorded regularly. Random and fasting blood glucose levels were determined regularly using a Precision Xceed glucometer and Precision XtraPlus test stripes (Abbott). Intravenous glucose tolerance, homeostasis model assessment of β -cell function, and homeostasis model assessment of insulin resistance were determined as described previously (9,10). Continuous glucose monitoring was performed using the Guardian REAL-Time System (Medtronic) whereby a glucose sensor was inserted subcutaneously behind the ear and data were transferred via a connected transmitter to an external computer. Plasma insulin levels were determined by radioimmunoassay (Millipore). Insulin-treated pigs received a combination of long-acting insulin (Lantus; Sanofi) and short-acting insulin (NovoRapid; NovoNordisk). Blood glucose levels were determined once or twice daily using a glucometer to control treatment.

Necropsy, pancreas sampling, quantitative stereological analyses, and electron microscopy. The 8-day-old and 4.5-month-old pigs were killed and subjected to routine necropsy. Selected organs were weighed. Pancreas samples for quantitative stereological analyses were chosen by systematic random sampling and were routinely processed for paraffin histology (9). β -cells and non- β -cells were visualized as described (9) using a polyclonal guinea pig antiporcine insulin antibody or polyclonal rabbit anti-human glucagon, somatostatin, and pancreatic polypeptide antibodies, respectively. The volume densities and the total volumes of β -cells and non- β -cells were determined as described previously (9). For transmission electron microscopy of β -cells, pancreas samples were fixed in 6.25% glutaraldehyde in Sorensen phosphate buffer (pH 7.4) for 24 h and processed as described (3). The left kidney was fixed by orthograde vascular perfusion with 4% formaldehyde. Six specimens of the renal cortex obtained by systematic random sampling (11) were processed for plastic embedded light microscopy (11) and transmission electron microscopy as described previously (11). The mean glomerular volume was determined from the mean glomerular profile area, as described (11). The true harmonic mean thickness of the glomerular basement membrane (GBM) was determined by the orthogonal intercept method (11). Tibial nerve

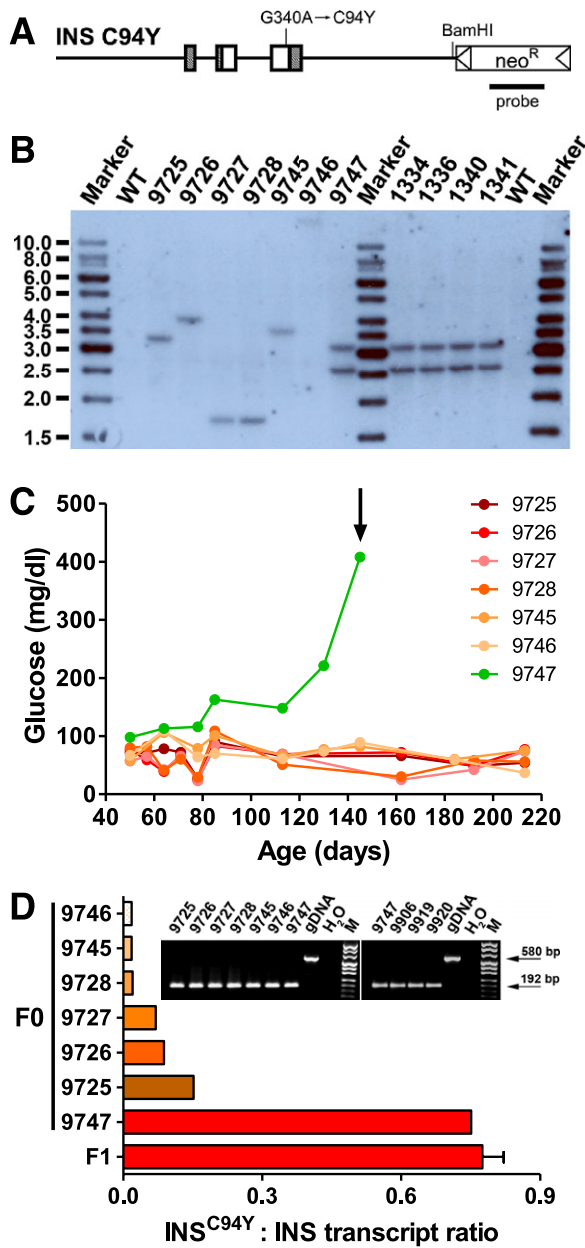


FIG. 1. Generation of diabetic *INS*^{C94Y} transgenic (tg) pigs (expression construct, Southern blot, glucose levels, transgene expression). **A:** Expression cassette including the porcine *INS* gene with the Cys→Tyr exchange at amino acid position 94, essential regulatory elements, and a neomycin selection cassette (*neo*). Restriction site of *Bam*HI and binding site of the probe (bar) used for Southern blot analysis are indicated. **B:** Southern blot analysis of *Bam*HI digested genomic DNA from *INS*^{C94Y} tg pigs and littermate control animals (wt) showing different integration sites in founders 9725, 9726, 9727, 9728, 9745, 9746, and 9747. Tg offspring (1334, 1336, 1340, 1341) of founder 9747 show the same integration pattern as founder 9747, demonstrating a single integration site. **C:** Fasting blood glucose levels of *INS*^{C94Y} tg founder boars showing hyperglycemia in founder 9747 progressively deteriorating over time; arrow indicates start of insulin therapy. **D:** Quantification of *INS*^{C94Y} and wt *INS* transcripts in pancreatic tissue of *INS*^{C94Y} tg pigs by next-generation sequencing of RT-PCR amplicons. Founder 9747 shows at least five-fold higher expression of the mutant *INS*^{C94Y} compared with the other six founders (F0) and similar expression compared with its F1 offspring (F1; *n* = 3). *Inset:* RT-PCR products of *INS*^{C94Y}/*INS* transcripts in pancreatic tissue of all *INS*^{C94Y} tg founders (*left*) and founder 9747, as well as its offspring (*right*). M, pUC Mix Marker; gDNA, genomic DNA; H₂O, Aqua bidest.

fascicles were immersed in 2.5% glutaraldehyde in Soerensen phosphate buffer (pH 7.4) for 1 h and postfixed in 2% OsO₄ for 2 h. After a graded alcohol series, they were embedded in epoxy resin. Semithin sections (0.5 μm) were stained with azur II-methylene blue-safranin. Some nerve fascicles were prepared for fiber teasing as reported previously (12).

Statistics. All data are presented as means ± SEM unless indicated otherwise. Longitudinal data of blood glucose levels and body weight gain were statistically evaluated by ANOVA (PROC MIXED; SAS 8.2), taking the fixed effects of group (transgenic versus control) and age as well as the random effect of animal into account (9). For other parameters, the two-tailed unpaired Mann-Whitney *U* test in combination with an exact test procedure (SPSS 19.0) or two-tailed unpaired Student *t* test was used unless indicated otherwise. *P* < 0.05 was considered significant.

RESULTS

Generation of *INS*^{C94Y} transgenic pigs. A total of 562 embryos reconstructed from *INS*^{C94Y} nucleofected cell clones were transferred to five recipient gilts, resulting in three pregnancies, two of which went to term. Southern blot analysis revealed that all seven offspring were *INS*^{C94Y} transgenic, with different transgene integration patterns (Fig. 1B). Founder boar 9747 exhibited elevated fasting blood glucose levels at the age of 85 days, further increasing with age. The boar showed distinct growth restriction, which could be substantially improved by insulin treatment. Transgenic offspring were delivered after mating 9747 to wild-type sows and showed the same transgene integration pattern as the sire, arguing for a single integration site in the genome. The other six *INS*^{C94Y} transgenic founder boars had normal development and exhibited unaltered glucose levels (Fig. 1C) and intravenous glucose tolerance (data not shown) within the observation period of 213 days. The *INS*^{C94Y}-to-*INS* transcript ratios in pancreas samples of 9747 and his diabetic offspring (*n* = 3) were 0.75 and 0.78 ± 0.05. In the other founder boars, this ratio was at least five-fold lower (Fig. 1D), indicating that the diabetogenic effect of *INS*^{C94Y} is dose dependent.

Glucose control and insulin secretion. To evaluate the effect of *INS*^{C94Y} expression on glucose homeostasis, blood glucose levels were measured regularly beginning at birth before the first food intake. Transgenic offspring exhibited significantly (*P* < 0.05) elevated random blood glucose levels within 24 h after birth compared with their nontransgenic littermates (Fig. 2A). However, divergence in basal plasma insulin levels of 8-day-old *INS*^{C94Y} transgenic pigs compared with controls was less pronounced (Fig. 2B). In contrast, fasting insulin levels of 4.5-month-old *INS*^{C94Y} transgenic pigs were significantly (*P* < 0.01) reduced compared with nontransgenic littermates (Fig. 2B). Homeostasis model of assessment of β-cells index was significantly reduced in 4.5-month-old *INS*^{C94Y} transgenic pigs (1.8 ± 0.4 vs. 47.2 ± 10.5; *P* < 0.01, one-tailed), indicating reduced steady-state β-cell function. Homeostasis model of assessment of insulin resistance index was significantly elevated in 4.5-month-old *INS*^{C94Y} transgenic pigs (2.4 ± 0.48 vs. 1.2 ± 0.24; *P* < 0.05, one-tailed), suggesting insulin resistance. For long-term survival, *INS*^{C94Y} transgenic pigs were treated with insulin starting at the age of 4.5 months. Glucose control under insulin treatment was evaluated over a period of 42 h, and the average blood glucose concentration in the *INS*^{C94Y} transgenic pigs was 123.2 ± 41.9 (SD) vs. 92 ± 11.9 (SD) mg/dL in the control pigs (Fig. 2C). Variations in blood glucose levels were generally greater in the *INS*^{C94Y} transgenic (40–198 mg/dL) than in the control pigs (62–114 mg/dL).

Loss of β-cell mass and ultrastructural alterations in β-cells. Pancreas weight did not differ between *INS*^{C94Y} transgenic pigs and controls at 8 days of age (4.4 ± 0.6 vs.

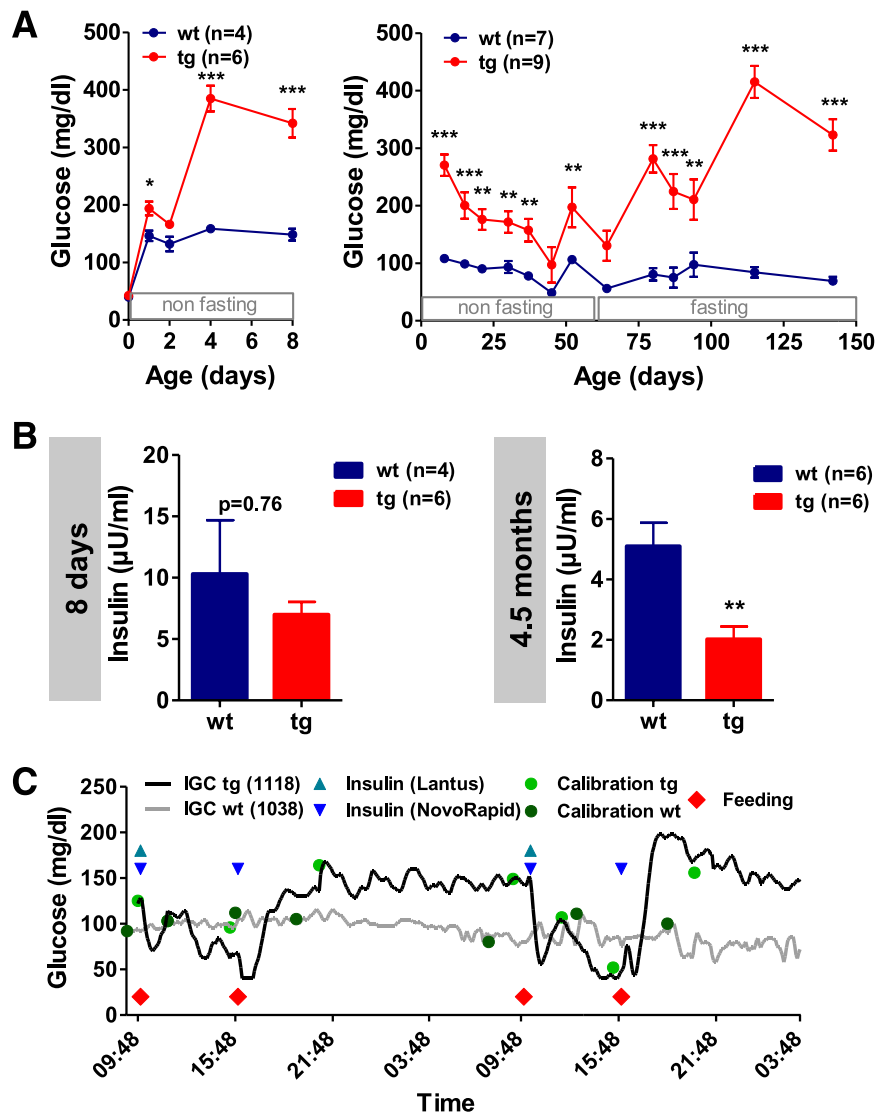


FIG. 2. Glucose control and insulin secretion in *INS*^{C94Y} transgenic (tg) pigs. **A:** Random blood glucose levels (*left*) of *INS*^{C94Y} tg pigs and littermate controls (wt) up to age 8 days. Glucose levels of tg pigs are significantly elevated 24 h after birth. Random and fasting blood glucose levels (*right*) of tg and wt pigs show deterioration of glucose control in tg pigs with increasing age. **B:** Fasting insulin levels of 8-day-old and 4.5-month-old *INS*^{C94Y} tg pigs and littermate controls reveal hypoinsulinemia in 4.5-month-old *INS*^{C94Y} tg pigs vs. littermate controls. **C:** The 42-h continuous glucose monitoring of an insulin-treated *INS*^{C94Y} tg pig and a nontransgenic control (wt) pig. Insulin dose per day: 0.5 to 1 units per kilogram of body weight. IGC, interstitial glucose concentration. Data are means \pm SEM. * $P < 0.05$; ** $P < 0.01$; *** $P < 0.001$ vs. control.

4.9 ± 0.4 g; $P = 0.5$) but was significantly reduced in 4.5-month-old *INS*^{C94Y} transgenic pigs compared with nontransgenic littermates (79 ± 6 vs. 134 ± 5 g; $P = 0.001$), proportionate with body weight reduction. Qualitative histological evaluation of the pancreas revealed single β -cells and small islet clusters in 8-day-old *INS*^{C94Y} transgenic pigs to the same extent as in controls (Fig. 3A). Compared with nontransgenic littermates, pancreas sections of 4.5-month-old *INS*^{C94Y} transgenic pigs revealed a visibly reduced β -cell mass and insulin immunostaining intensity (Fig. 3A). The volume density and total volume of β -cells in the pancreas of 8-day-old *INS*^{C94Y} transgenic pigs were unaltered compared with controls. However, in 4.5-month-old *INS*^{C94Y} transgenic pigs, the volume density of β -cells in the pancreas, total volume, and the total volume of β -cells related to body weight were diminished by 54, 72, and 53%, respectively (Fig. 3B). Electron microscopy revealed unaltered secretory granules but dilation of the ER in 8-day-old transgenic piglets and a low number of

insulin secretory granules and severe dilation of the ER in β -cells of 4.5-month-old transgenic pigs (Fig. 3C). The volume density of non- β -cells in the pancreas was not altered in 4.5-month-old *INS*^{C94Y} transgenic pigs. The total non- β -cell volume of *INS*^{C94Y} transgenic pigs was reduced by 38% (290 ± 39 vs. 472 ± 59 mm³; $P < 0.05$); however, in relation to body weight, their total non- β -cell volume was not different from that of controls (6.5 ± 0.8 vs. 6.0 ± 0.5 ; $P = 0.9$).

Secondary alterations. *INS*^{C94Y} transgenic pigs grew normally up to an age of 2 months; thereafter, their growth rate decreased, resulting in a 41% lower body weight at the age of 4.5 months (Fig. 4A). The weights of most organs, including the pancreas, were proportionately reduced (data not shown). A notable exception was kidney weight, which was reduced by only 15%. Thus, relative kidney weight was significantly increased (Fig. 4B). Further, the ratio of glomerular volume to body weight was significantly increased in 4.5-month-old *INS*^{C94Y} transgenic pigs

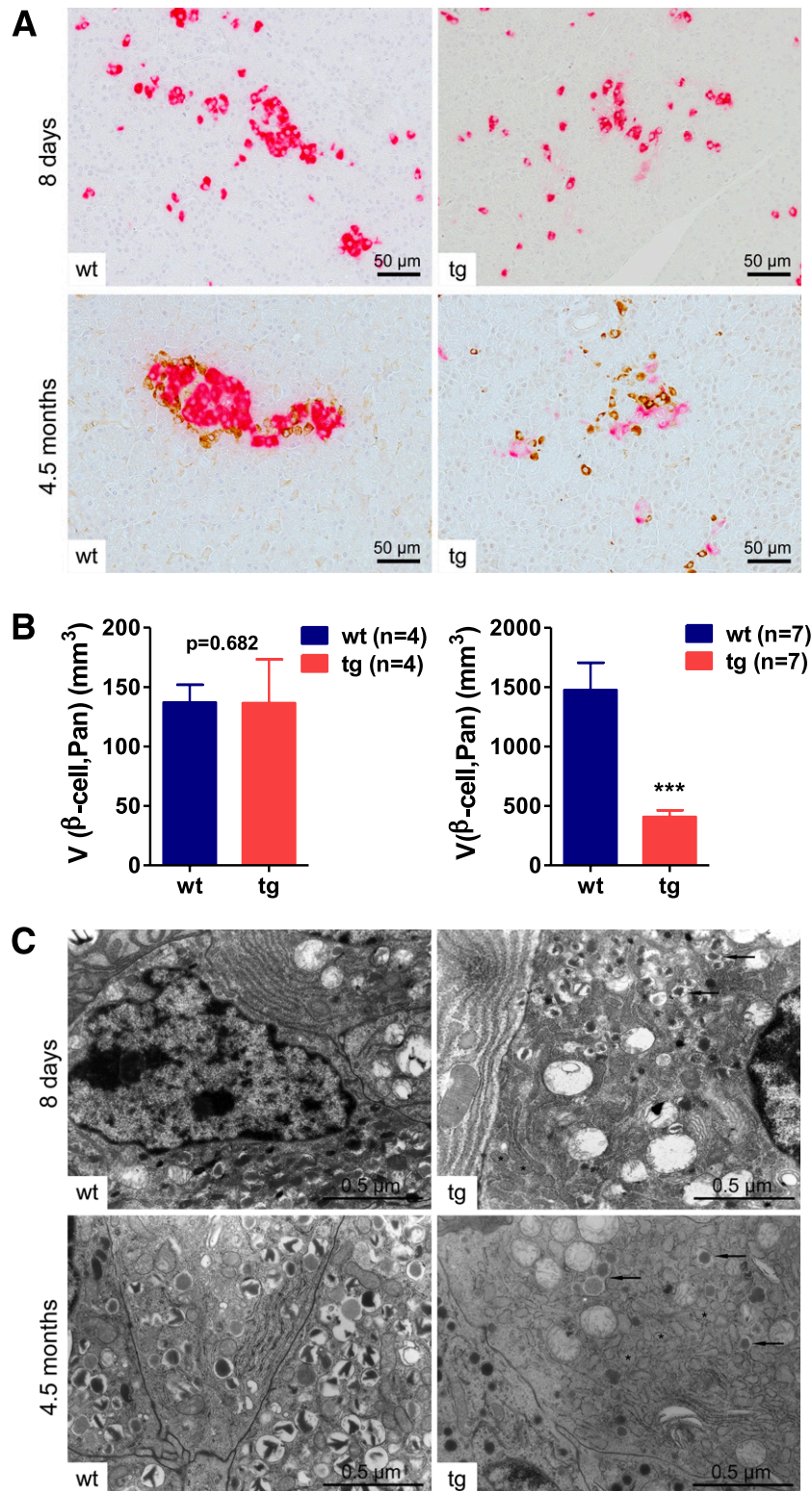


FIG. 3. Reduced β -cell mass and ultrastructural changes in INS^{C94Y} transgenic (tg) pigs. **A:** Immunohistochemical staining for insulin in 8-day-old pigs and double immunohistochemical staining for insulin (pink) and glucagon, somatostatin, and pancreatic polypeptide (brown) in 4.5-month-old pigs. Representative histological sections of pancreatic tissue from a control (wt) and an INS^{C94Y} tg pig. Scale bar = 50 μ m. **B:** Quantitative stereological analyses of the pancreas. Unaltered total β -cell volume ($V_{(\beta\text{-cell, Pan})}$) in 8-day-old INS^{C94Y} tg pigs ($n = 4$ per group) and significant reduction of $V_{(\beta\text{-cell, Pan})}$ in 4.5-month-old INS^{C94Y} tg pigs ($n = 7$ per group) compared with littermate controls. Data are means \pm SEM. *** $P < 0.001$ vs. control. **C:** Transmission electron microscopy of pancreatic tissue from a representative 8-day-old and 4.5-month-old INS^{C94Y} tg and a littermate control (wt) pig. In 4.5-month-old INS^{C94Y} tg pigs, only a few insulin granules (arrows) and severe dilation of endoplasmic reticulum (*) are visible, whereas in 8-day-old tg pigs insulin granules are present and dilation of the endoplasmic reticulum is less severe.

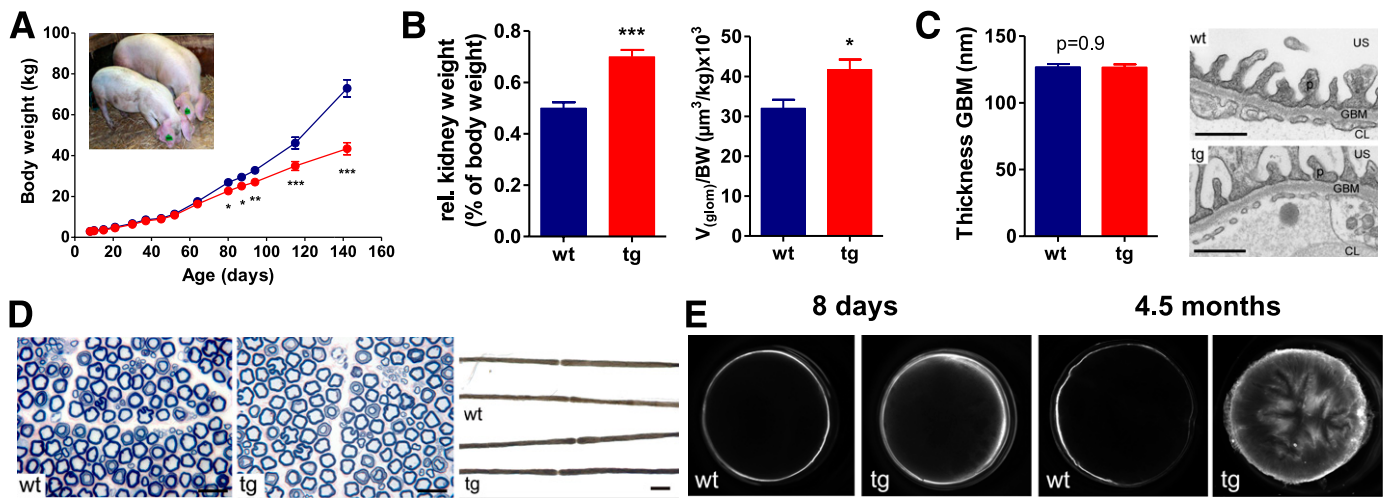


FIG. 4. Diabetes-related alterations of *INS*^{C94Y} transgenic (tg) pigs. **A:** Body weight gain in *INS*^{C94Y} tg pigs (red circles; $n = 9$) and controls (blue circles; $n = 7$) up to age 4.5 months. **B:** Increased relative (rel.) kidney weight (percent body weight) and ratio of mean glomerular volume to body weight ($V_{\text{glom}} / \text{BW} [\mu\text{m}^3/\text{kg}] \times 10^3$) in 4.5-month-old *INS*^{C94Y} tg pigs vs. littermate controls (wt; $n = 7$ per group). **C:** Unaltered true harmonic mean thickness of the GBM in 4.5-month-old *INS*^{C94Y} tg pigs compared with littermate controls ($n = 3$ per group) and representative transmission electron microscopic sections. Scale bar, 500 nm. **D:** Representative histological sections (left) of a tibial nerve fascicle of a 4.5-month-old *INS*^{C94Y} tg pig and a littermate control demonstrating unchanged fiber density without structural changes in axons and myelin. Azur II-methylene blue-safranin staining. Scale bar, 100 μm . Single fiber teasings (right) showing unchanged fiber myelination and morphology of nodes of Ranvier. Scale bar, 100 μm . **E:** Eye lenses of 8-day-old and 4.5-month-old *INS*^{C94Y} tg pigs and littermate controls (wt) show a progressive cataract with increasing opacity in tg pigs, whereas lenses of wt pigs remain clear. Data are means \pm SEM. * $P < 0.05$ vs. control; *** $P < 0.001$ vs. control. US, urinary space; CL, glomerular capillary lumen; p, podocyte foot process.

(Fig. 4B). However, there were no histological signs of diabetic kidney disease in 4.5-month-old diabetic pigs (Fig. 4C) or in 1-year-old cloned diabetic *INS*^{C94Y} transgenic pigs ($n = 5$; kindly provided by Minitube of America). Also, there was no histological evidence for diabetic neuropathy in 4.5-month-old *INS*^{C94Y} transgenic pigs (Fig. 4D). In contrast, cataract was observed at the edges of the eye lenses in 8-day-old *INS*^{C94Y} transgenic pigs, whereas at 4.5 months of age the entire lens was affected (Fig. 4E).

DISCUSSION

In this study, we established the first transgenic pig model of PNDM triggered by an *INS* mutation. Induction of insulin-deficient diabetes by other methods has substantial drawbacks. Chemical diabetes induction, e.g., by streptozotocin treatment, is hampered by variable outcomes, including age, sex, or individual differences in susceptibility or spontaneous reversal of diabetes (13). Pancreatectomy is highly invasive, time consuming, and expensive, and it requires supplementation of the pancreatic enzymes (14). In contrast, *INS*^{C94Y} transgenic pigs have development of stable diabetes because of a specific clinically relevant impairment of β -cells. Unaltered blood glucose levels and body weight at birth suggest postnatal disturbance of β -cells, although impairment of (pro)insulin action to some extent during fetal development cannot be excluded. Like the *Ins2* mutant mouse models, the *INS*^{C94Y} transgenic pig model does not reflect all disease mechanisms of human type 1 diabetes because of the lack of the autoimmune component. Importantly, *INS*^{C94Y} transgenic pigs can be propagated by conventional breeding when treated with insulin. However, the costs for maintenance of pigs (\$3.30 per animal and per day in our facility) and, in particular, of diabetic pigs (\$12 per day) are markedly higher than for rodent models.

Expression of *INS*^{C94Y} transcripts at a level of 75% of the endogenous *INS* mRNA was sufficient to cause hyperglycemia already in newborn transgenic pigs, whereas β -cell

mass was initially unaltered. Nevertheless, structural alterations of β -cells suggested ER stress already at this early stage. At the age of 4.5 months, ratio of β -cell mass to body weight of transgenic pigs was significantly reduced and was associated with marked ultrastructural evidence for loss of insulin granules and ER stress. Because insulin staining was used to identify β -cells, we may have overestimated the reduction of β -cell mass attributable to loss of insulin granules. Nevertheless, our findings indicate that the *INS*^{C94Y} transgenic pig model reflects the disease mechanisms demonstrated in *Ins2* mutant mice and imposed in human PNDM. Binding affinity of *INS*^{C94Y} might differ from endogenous INS, which possibly could have led to accompanying insulin resistance in cases of higher binding affinity of *INS*^{C94Y} (15). However, in vitro studies using *des* mutants of human insulin showed that each of the three disulfide bonds is essential for receptor binding affinity, and that lack of the A7B7 interchain disulfide bond has the greatest impact on binding affinity (16). In addition, it remains to be clarified if *INS*^{C94Y} is at all secreted from β -cells because in vitro studies suggest failure of *INS*^{C96Y} to undergo exocytosis in response to glucose (17–19) and that mutant misfolded proinsulin also affects bystander proinsulin in the ER (4).

The growth rate of untreated *INS*^{C94Y} transgenic pigs was markedly reduced as compared with controls. This is in line with stunted growth of diabetic children with insufficient insulin therapy (20) and underlines the essential role of insulin as growth factor and anabolic hormone. Whereas the weights of most organs of *INS*^{C94Y} transgenic pigs revealed proportional reduction in body weight, the relative kidney weight was increased by 29%. Renal and glomerular hypertrophy is a common early-stage finding in diabetic patients (21); however, histopathological examination did not reveal alterations diagnostic for diabetic nephropathy in *INS*^{C94Y} transgenic pigs. Whereas the thickness of the GBM is an early and sensitive indicator of diabetic kidney disease in mice (11), it takes years until

thickening of the GBM can be detected in human diabetic patients, and even longer until clinical diabetic nephropathy is present (22). Therefore, it is not surprising that GBM thickness is still unaltered in 4.5-month-old *INS*^{C94Y} transgenic pigs. Future studies need to address if time or complicating factors such as high-protein diet or elevated blood pressure (23) will provoke kidney lesions in diabetic *INS*^{C94Y} transgenic pigs.

The lack of kidney pathology in young *INS*^{C94Y} transgenic pigs is in contrast to findings in a diabetic transgenic pig model expressing mutant hepatocyte nuclear factor-1 α . Immature renal development and liver alterations were detected in two hepatocyte nuclear factor-1 α transgenic-cloned piglets, whereas two others revealed glomerular hypertrophy and sclerosis. Whether these lesions were attributable to the dominant-negative effects of mutant hepatocyte nuclear factor-1 α , secondary changes attributable to chronic hyperglycemia, or anomalies associated with somatic cell nuclear transfer remains unclear (24). Structural changes in peripheral nerves possibly will develop with increasing age in *INS*^{C94Y} transgenic pigs because chronic sensorimotor diabetic polyneuropathy is highly dependent on diabetes duration in humans (25). Similar to humans, *INS*^{C94Y} transgenic pigs have development of remarkable cataracts, which never has been reported in *Ins2* mutant mice. This might be related to a lower aldose reductase activity in lenses of mice compared with humans and rats (26). Therefore, pigs seem to be a favorable model for diabetic cataracts, although the underlying molecular mechanism has to be clarified.

A number of interesting questions can be addressed with this novel pig model for PNDM. A genetically diabetic pig model facilitates testing the functionality of transplanted pancreatic islets, e.g., after microencapsulation or in specific macrodevices (27), in an organism of human size. Also, *INS*^{C94Y} transgenic pigs seem to be a valuable model for preclinical testing of novel treatment strategies to improve glucose control. The reproducible loss of β -cells makes the *INS*^{C94Y} transgenic pig an attractive model for the development of in vivo imaging techniques to monitor β -cell mass. Developmental consequences of maternal diabetes on oocytes and embryos and their interaction with the maternal environment are other interesting research topics. Because of the similarities in oocyte maturation and early development of human and pig embryos (28), the *INS*^{C94Y} transgenic pig is an attractive model to address these questions.

ACKNOWLEDGMENTS

This study was supported by the Federal Ministry of Education and Research (Leading-Edge Cluster m⁴-Personalized Medicine and Targeted Therapies), by the Diabetes Hilfs- und Forschungsfonds Deutschland (DHFD), by the DFG Transregio Collaborative Research Center 127 "Biology of xenogeneic cell, tissue and organ transplantation—from bench to bedside," and by BioSysNet. C.B.-R. received a research scholarship from the Elite Network of Bavaria.

No potential conflicts of interest relevant to this article were reported.

S.R. researched data, contributed to discussion, and wrote the manuscript. C.B.-R., A.Bl., D.E., E.S., A.W., B.K., M.K., A.Bä., S.K., and O.P. researched data, contributed to discussion and reviewed and edited the manuscript. N.H., N.K., H.N., J.G., H.B., R.W., and E.W. contributed to discussion and reviewed and edited the manuscript. E.W. and S.R. are

the guarantors of this work and, as such, had full access to all the data in the study and take responsibility for the integrity of the data and the accuracy of the data analysis.

Parts of this study were presented at the Swine in Biomedical Research Conference, Chicago, Illinois, 17–19 July 2011; the XXIV Congress of the Transplantation Society (TTS), Berlin, Germany, 15–19 July 2012; and at the 48th meeting of the European Association for the Study of Diabetes (EASD), Berlin, Germany, 1–5 October 2012.

The authors thank Heinrich Flaswinkel (Chair for Molecular Animal Breeding and Biotechnology, Ludwig Maximilian University Munich, Munich, Germany) for providing the construct. The authors thank Miwako Kösters (Laboratory for Functional Genome Analysis, Ludwig Maximilian University Munich, Munich, Germany), Angela Siebert (Institute of Veterinary Pathology at the Centre for Clinical Veterinary Medicine, Ludwig Maximilian University Munich, Munich, Germany), and Lisa Pichl (Institute of Veterinary Pathology at the Centre for Clinical Veterinary Medicine, Ludwig Maximilian University Munich, Munich, Germany), as well as Elfi Holupirek, Christian Erdle, and Siegfried Elsner (Molecular Animal Breeding and Biotechnology, Ludwig Maximilian University Munich, Munich, Germany) for excellent technical assistance and animal management. Minitube of America is gratefully acknowledged for providing kidney samples from 1-year-old cloned *INS*^{C94Y} transgenic pigs.

REFERENCES

1. Støy J, Edghill EL, Flanagan SE, et al.; Neonatal Diabetes International Collaborative Group. Insulin gene mutations as a cause of permanent neonatal diabetes. *Proc Natl Acad Sci USA* 2007;104:15040–15044
2. Yoshioka M, Kayo T, Ikeda T, Koizumi A. A novel locus, Mody4, distal to D7Mit189 on chromosome 7 determines early-onset NIDDM in nonobese C57BL/6 (Akita) mutant mice. *Diabetes* 1997;46:887–894
3. Herbach N, Rathkolb B, Kemter E, et al. Dominant-negative effects of a novel mutated *Ins2* allele causes early-onset diabetes and severe beta-cell loss in Munich *Ins2*C95S mutant mice. *Diabetes* 2007;56:1268–1276
4. Hodish I, Liu M, Rajpal G, et al. Misfolded proinsulin affects bystander proinsulin in neonatal diabetes. *J Biol Chem* 2010;285:685–694
5. Oyadomari S, Koizumi A, Takeda K, et al. Targeted disruption of the Chop gene delays endoplasmic reticulum stress-mediated diabetes. *J Clin Invest* 2002;109:525–532
6. Fonseca SG, Burcin M, Gromada J, Urano F. Endoplasmic reticulum stress in beta-cells and development of diabetes. *Curr Opin Pharmacol* 2009;9:763–770
7. Allen JR, Nguyen LX, Sargent KE, Lipson KL, Hackett A, Urano F. High ER stress in beta-cells stimulates intracellular degradation of misfolded insulin. *Biochem Biophys Res Commun* 2004;324:166–170
8. Klymiuk N, Bocker W, Schonitzer V, Bahr A, Radic T, Frohlich T, Wunsch A, Kessler B, Kurome M, Schilling E, Herbach N, Wanke R, Nagashima H, Mutschler W, Arnold GJ, Schwinzer R, Schieker M, Wolf E. First inducible transgene expression in porcine large animal models. *FASEB J* 2012;26:1086–1099
9. Renner S, Fehlings C, Herbach N, et al. Glucose intolerance and reduced proliferation of pancreatic beta-cells in transgenic pigs with impaired glucose-dependent insulinotropic polypeptide function. *Diabetes* 2010;59:1228–1238
10. Renner S, Römisch-Margl W, Prehn C, et al. Changing metabolic signatures of amino acids and lipids during the prediabetic period in a pig model with impaired incretin function and reduced β -cell mass. *Diabetes* 2012;61:2166–2175
11. Herbach N, Schairer I, Blutke A, et al. Diabetic kidney lesions of GIPRdn transgenic mice: podocyte hypertrophy and thickening of the GBM precede glomerular hypertrophy and glomerulosclerosis. *Am J Physiol Renal Physiol* 2009;296:F819–F829
12. Wieczorek LA. *Nervenzupfpräparation (nerve fiber teasing) in der Diagnostik peripherer Neuropathien beim Tier: Methodik und Interpretation*. München, LMU München, 2002 [in German]
13. Dufrane D, van Steenberghe M, Guiot Y, Goebbels RM, Saliez A, Gianello P. Streptozotocin-induced diabetes in large animals (pigs/primates): role of GLUT2 transporter and beta-cell plasticity. *Transplantation* 2006;81:36–45

14. Stump KC, Swindle MM, Saudek CD, Strandberg JD. Pancreatectomized swine as a model of diabetes mellitus. *Lab Anim Sci* 1988;38:439–443
15. Taylor SI, Hedvo JA, Underhill LH, Kasuga M, Elders MJ, Roth J. Extreme insulin resistance in association with abnormally high binding affinity of insulin receptors from a patient with leprechaunism: evidence for a defect intrinsic to the receptor. *J Clin Endocrinol Metab* 1982;55:1108–1113
16. Chang SG, Choi KD, Jang SH, Shin HC. Role of disulfide bonds in the structure and activity of human insulin. *Mol Cells* 2003;16:323–330
17. Colombo C, Porzio O, Liu M, et al.; Early Onset Diabetes Study Group of the Italian Society of Pediatric Endocrinology and Diabetes (SIEDP). Seven mutations in the human insulin gene linked to permanent neonatal/infancy-onset diabetes mellitus. *J Clin Invest* 2008;118:2148–2156
18. Liu M, Li Y, Cavener D, Arvan P. Proinsulin disulfide maturation and misfolding in the endoplasmic reticulum. *J Biol Chem* 2005;280:13209–13212
19. Rajan S, Eames SC, Park SY, et al. In vitro processing and secretion of mutant insulin proteins that cause permanent neonatal diabetes. *Am J Physiol Endocrinol Metab* 2010;298:E403–E410
20. Tattersall RB, Pyke DA. Growth in diabetic children. Studies in identical twins. *Lancet* 1973;2:1105–1109
21. Bilous R. *Diabetic Nephropathy*. Chichester, UK, John Wiley & Sons, Ltd, 2001
22. Pagtalunan ME, Miller PL, Jumping-Eagle S, et al. Podocyte loss and progressive glomerular injury in type II diabetes. *J Clin Invest* 1997;99:342–348
23. Zatz R, Meyer TW, Rennke HG, Brenner BM. Predominance of hemodynamic rather than metabolic factors in the pathogenesis of diabetic glomerulopathy. *Proc Natl Acad Sci USA* 1985;82:5963–5967
24. Umeyama K, Watanabe M, Saito H, et al. Dominant-negative mutant hepatocyte nuclear factor 1alpha induces diabetes in transgenic-cloned pigs. *Transgenic Res* 2009;18:697–706
25. Tesfaye S, Chaturvedi N, Eaton SE, et al.; EURODIAB Prospective Complications Study Group. Vascular risk factors and diabetic neuropathy. *N Engl J Med* 2005;352:341–350
26. Petrash JM. All in the family: aldose reductase and closely related aldose-keto reductases. *Cell Mol Life Sci* 2004;61:737–749
27. Ludwig B, Rotem A, Schmid J, et al. Improvement of islet function in a bioartificial pancreas by enhanced oxygen supply and growth hormone releasing hormone agonist. *Proc Natl Acad Sci USA* 2012;109:5022–5027
28. Prather RS, Ross JW, Isom SC, Green JA. Transcriptional, post-transcriptional and epigenetic control of porcine oocyte maturation and embryogenesis. *Soc Reprod Fertil Suppl* 2009;66:165–176